Earth Reinforcement, Ochiai, Yasufuku & Omine (eds) © 1996 Balkema, Rotterdam. ISBN 90 5410 833 9

Creep behavior of laboratory embankment reinforced with geogrid

H. Furuya, M. Toriihara & K. Hirama
Obayashi Corporation, Tokyo, Japan

ABSTRACT: In order to investigate long-term stabilization of embankment structure reinforced with geogrids, it is important to elucidate not only creep characteristic of geogrid but also creep behavior of whole reinforced embankment using geogrid by loading for a long time. This time, the authors have conducted laboratory slope model tests which are stage loading (3 steps) extending for a long time, in order to make clear the modified characteristics that are by means of creep, of reinforced embankment. The creep model tests were conducted considering both setting up the length of geogrids and layer number of them as a parameter.

Based on these observations of these test, they were found that the increase of not only transformation of reinforced embankment but also strain of geogrid laying in the model embankment considering as a creep ingredient. And the range of increase was recorded so remarkably as to load large degree of weight. Moreover, the increasing strain speed of the geogrid changed the length of them laying in the embankment, but it was constant in spite of the layer number of geogrids under laying same length of them, and it was admitted the tendency that the creep ingredient for long-term loading was getting smaller as time passed. And also the tendency was well explained by FEM analysis. This paper summarizes these results.

1 INTRODUCTION

When designing a long-term banking structure reinforced by geotextile, it must be assumed that in addition to the dead load of the fill-up ground, the long-term load also has an important effect. When considering the long-term stability of a banking structure reinforced by geotextile, it is important to understand not only the creep characteristics of the geogrids but also the creep behavior of the reinforced fill-up ground resulting from long-term loading.

A long-term loading test based on a fixed load was executed using internal slope model equipment to clarify the characteristics of the deformation caused by creep of the reinforced banking. Also, an FEM simulation of these tests was analyzed.

2 OUTOLINE OF CREEP TESTS

Table 1 shows the specifications of the geogrids and soil used in the creep model tests. The model slope creates the banking as shown in Figure 1 and Table 2 in a $2{,}000 \times 1{,}000 \times 300mm$ soil container; the side friction was reduced using silicone grease and a teflon sheet. Weights of *280 kg* each were used to load 3-step stairs at *22.6KPa* per step.

Table 1 Materials used in this Test

Geogrid	Polymer grid $Tmax = 16.67 \times 29.43kN/m, \ \varepsilon = 14\%$ $mesh: 28 \times 40mm$
Soil(sand)	Kinugawa Sand $\gamma t = 15.1kN/m^3 (Dr = 80\%)$ $w = 5\%, \ \phi = 33.2°$
Grill Frame	Aluminum $60 \times 30cm(mesh: 10cm)$

In Test 1, a test was made using the laying length of the geogrid as a parameter. The number of laid layers was three, and the laying lengths of the geogrids were *30, 50,* and *70 cm.*

In Test 2, a test was made using the number of laid layers of the geogrid as a parameter. The laying lengths of the geogrids were *3, 5,* and *7.*

The grill frame and the geogrids were joined. A distortion gages were attached to the geogrids to measure the tension distribution at loading. The distortion of the fill-up ground was measured by analyzing photographs using a displacement meter and gages.

Table 2 Test Case

	Test-1			Test-2		
Test Case No.	1	2	3	4	5	6
Number of Layer (n)	3	3	3	3	5	7
Length of Geogrid (cm)	30	50	70	70	70	70

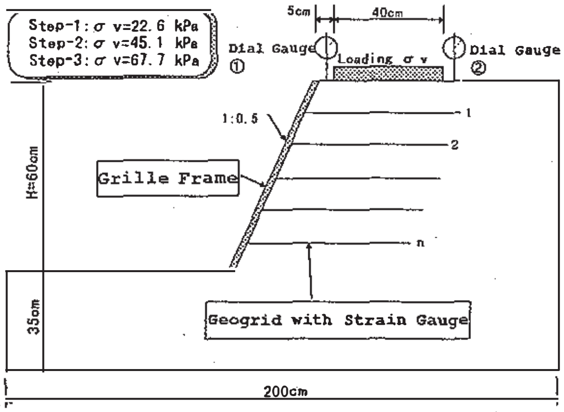

Figure 1 Profile of the Creep Test

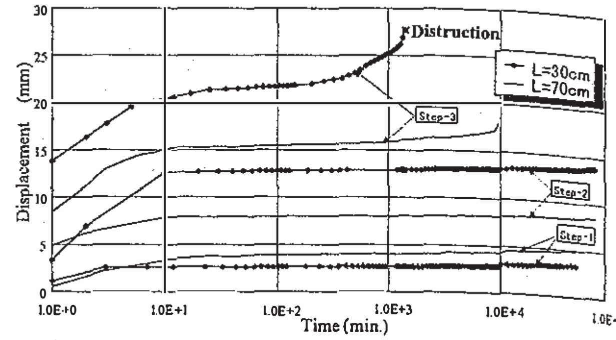

Figure 2 Displacement of Dial Gauge ①

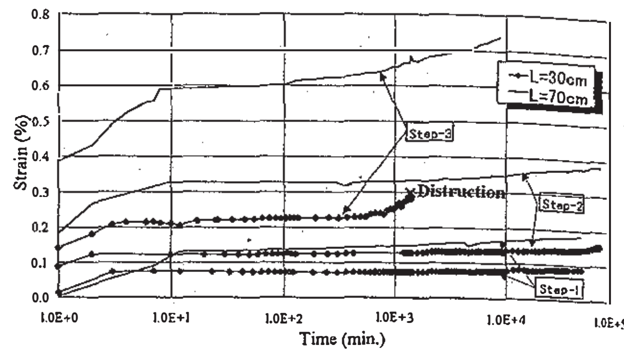

Figure 3 Strain of Geogrid (Peak of 1st Layer)

3 TEST RESULTS AND CONSIDERATIONS

3.1 TEST 1: Test Using the Laying Length as a Parameter

Figure 2 shows the aging of the displacement meter installed on top of the model slope when the laying lengths of the geogrids were *30* and *70 cm*. In loading steps 2 and 3, it is clear that the deformation of the geogrids with a longer laying length is reduced, and there is a clear difference in the reinforcement effect. There was a sudden increases in slope deformation (settlement) up to about *10 minutes* immediately after loading, then the slope entered a state of balance. Subsequently, there was a slight creep deformation of the fill-up ground, the extent of which depended on the load strength and laying length.

Figure 3 shows aging of distortion at the position where the distortion gage attached to the first-layer of the geogrid from the upper row of laying lengths *30* and *70 cm* showed the peak value. The increase in distortion immediately after loading showed the same trend as the displacement meter on top of the

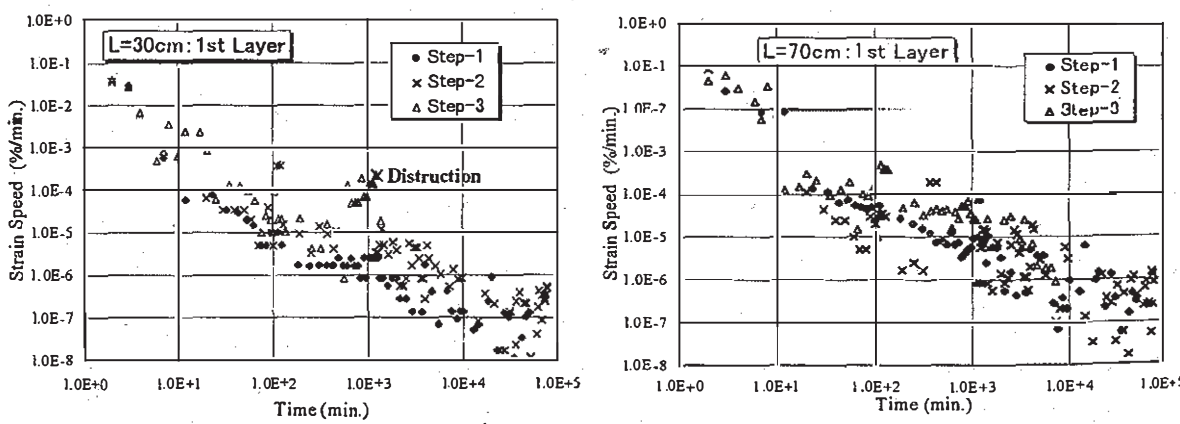

Figure 4 Relationship between Distortion Speed and Time (1)

banking slope. In loading steps 1 and 2, creep behavior slowly appeared in the vicinity after *1,000 minutes*. In step 3, the distortion increased after about *100 minutes*. This trend is remarkable in the geogrid with a longer laying length, and the absolute distortion generated is also large.
This indicates that the geogrid with the longer laying length has a higher resistance against slope shear deformation than that having a shorter laying length.

Figure 4 shows the relationship between the distortion speed and elapsed time for the geogrid at the position indicated in Figure 3. The rate of distortion immediately after loading decreased suddenly, and showed almost the same trend up to step 2, independent of the laying length of the geogrid. It is assumed that this is because the differences in resistance of the geogrids are not fully exposed by a small loading, and thus the deformation characteristics of the reinforcing fill-up ground depends on the strength of the banking material. However, in step 3, large differences in deformation characteristics for different laying lengths were observed.

3.2 TEST 2: Test Using the Number of Laid Layers as a Parameter

Figure 5 shows the aging of the displacement meter installed on top of the model slope when the number of laid layers of geogrids were 3 and 7. The displacement was larger in the 3-layered geogrid than in the 7-layered one.

Both under went rapid displacement for up to about *6 minutes* immediately after loading and then entered a state of balance. Subsequently, the deformation of the fill-up ground showed creep behavior in each loading step. In loading step 2 in particular, the deformation increased in both the 3-layered and 7-layered geogrids for up to *6,000 minutes* after loading. In loading step 3, the deformation of the banking of the 3-layered geogrid increased rapidly during the first *720 minutes* after loading. This caused the surface layer to collapse, effectively terminating the test.

Figure 6 shows the aging of the peak distortion generated in the geogrid at the central part (second

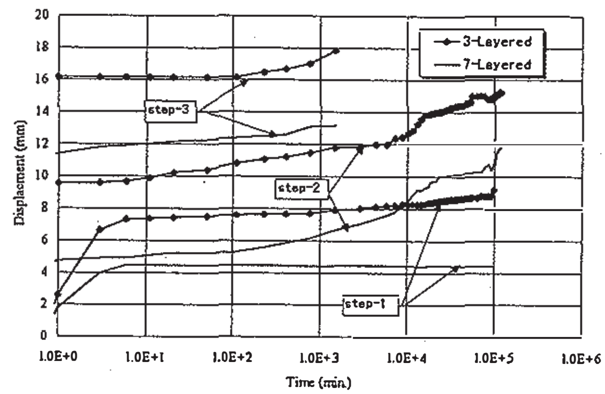

Figure 5 Displacement of Dial Gauge ①

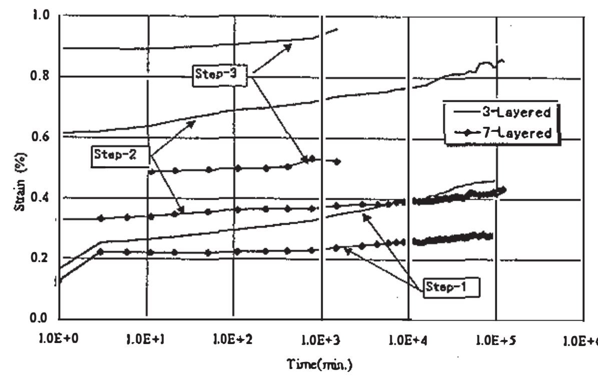

Figure 6 Strain of Geogrid
[3-Layered Model : Peak of 2nd Layer]
[7-Layered Model : Peak of 4th Layer]

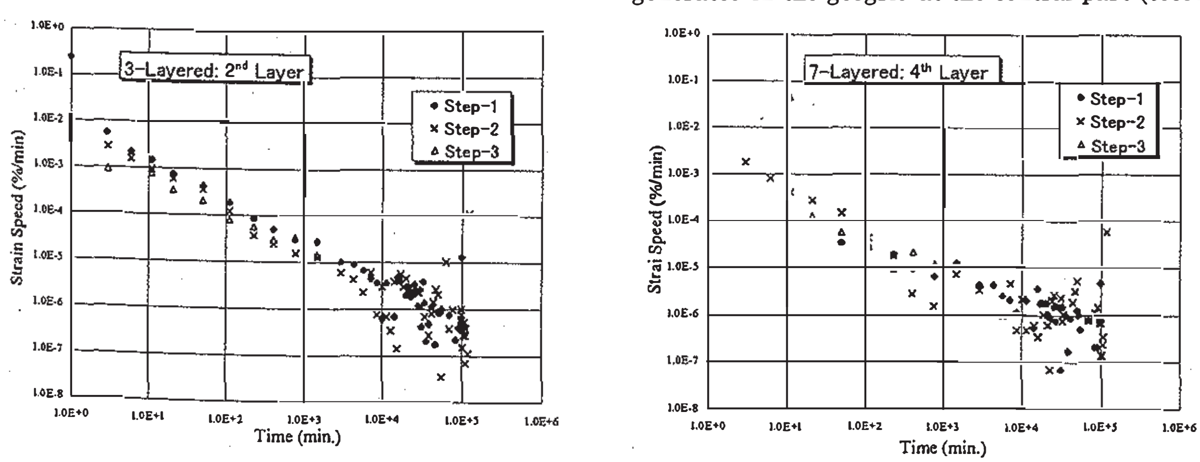

Figure 7 Relationship between Distortion Speed and Time (2)

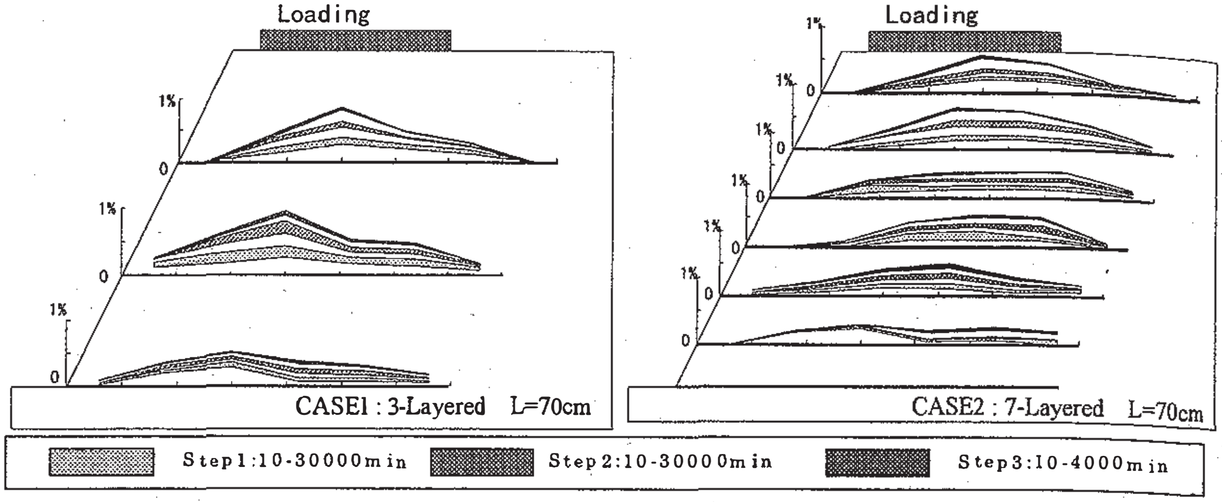

Figure 8 The Distribution of the Distortion

layer from the top for the 3-layered model, and fourth layer from the top for the 7-layered model) of the banking height. The distortion generated in the geogrid was larger in the 3-layered model than in the 7-layered one.

The increase in distortion immediately after loading showed the same trend as the displacement meter on top of the banking slope. However, the creep behavior of subsequent elongation was more gentle in each loading step than the deformation of the fill-up ground. These results show that the reinforced banking with many laid layers has a large reinforcement effect and deformation suppression effect.

Figure 7 shows the relationship between the distortion speed and elapsed time for the reinforcing material at the position indicated in Figure 6. The rate of distortion immediately after loading decreased suddenly, and showed almost the same trend up to step 2.

Figure 8 also shows the distribution of the distortion generated in the geogrid at the start and end of each loading step for the 3-layered and 7-layered geogrids. The shaded portion in Figure 8 is assumed to be an increase in distortion caused by the creep in each loading step. This increment is larger in the 3-layered geogrid.

4 SIMULATION BY FEM

Based on the results of the tests described above, the results of the tests and an FEM analysis were compared for the 3-layered and 7-layered geogrids with a laying length of *70 cm*.

4.1 Analytical Model

In this analysis, the geogrid was modeled using visco-elastic elements in which creep phenomena

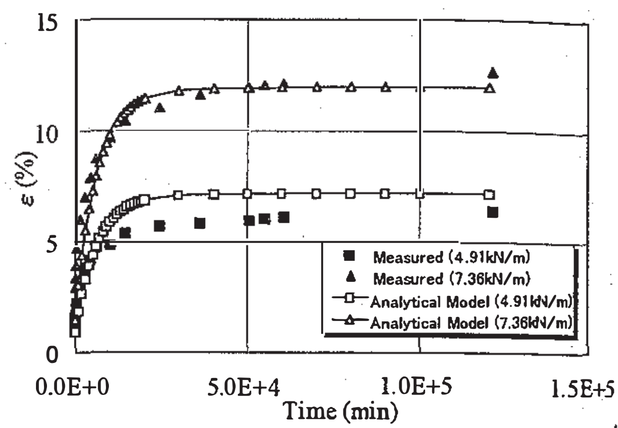

Figure 9 Comparison with Creep Test and Analytical Model

were considered, and the sand ground and grill frame were modeled using linear elastic elements.

For the geogrid, the formula used to relate the stress, distortion, and time is as follows:

$$\varepsilon(t) = J(t)\cdot\sigma(0) + \int_0^t J(t-t')\frac{d\sigma(t')}{dt'}dt' \quad \text{--- (1)}$$

In the creep test for the geogrid, the viscous flow can be ignored if the load is applied instantaneously when the distortion speed caused by the creep converges over time. Therefore, Formula (1) can be made discrete as follows:

$$\varepsilon(t) = J(t)\cdot\sigma_0, \quad J(t) = J_0 + \sum_{i=1}^{n} J_i\cdot(1 - e^{-t/T_i}) \quad \text{--- (2)}$$

Where, J_i is the creep compliance (*1/Kpa*) and T_i is the delay time (*min*). When the rate of change of creep speed is negative, the delay spectrum can be obtained according to the method of Akagi et al., and both T_i and J_i can be determined. J_0 is the spring compliance at instantaneous loading and is $J_0 = 1 / E_0$ (*1/KPa*).

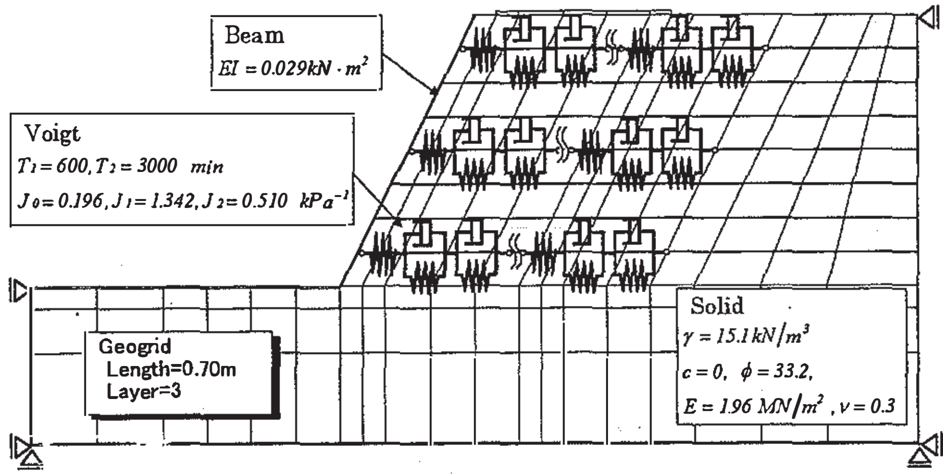

Figure 10 FEM Analytical Model

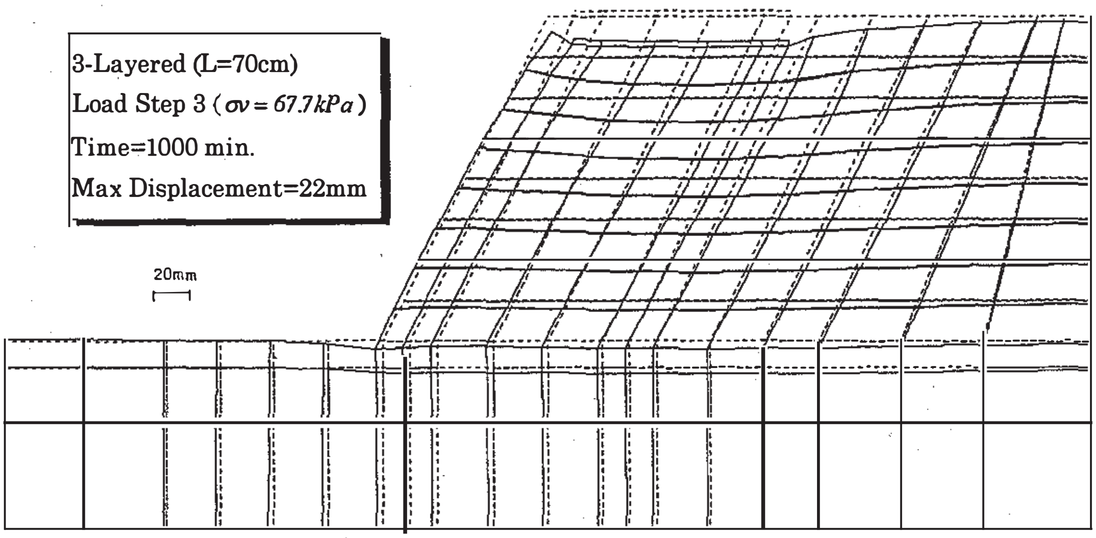

Figure 11 Deformation Diagram by FEM Analysis
(3-layered Model at Load Step 3)

The creep test data for the geogrid used in the test was interpolated, and the delay spectrum was obtained. Then, the results were used for the comparison. Figure 9 compares the creep test result (material test) for the geogrid and the calculated result obtained using the analytical model. The model simulates the creep characteristics of the geogrid with very good accuracy.

4.2 Analysis Results and Considerations

The creep model test was simulated using the visco-elastic model of the geogrid that was obtained using the method described above. Figure 10 shows the analytical model for the 3-layered geogrid and the constant used for the analysis.

Figure 11 shows deformation diagram of 3-layered model at load step-3. The vertical deformation is almost well explained by FEM analysis using this visco-elastic model of geogrid. But horizontal deformation by FEM analysis is little smaller than that of observation. This result is due to the slide between geogrids and soils.

Figures 12 and 13 show the aging of the peak distortion in the geogrid at the central part (second layer from the top for the 3-layered model, and fourth layer from the top for the 7-layered model) of the banking height, and the result obtained by FEM.

For the measured and analyzed values, the distortion in the geogrid is larger in the 3-layered model than in the 7-layered model in each loading step, layers, the reinforcement effect is larger and the deformation caused by creep is smaller.

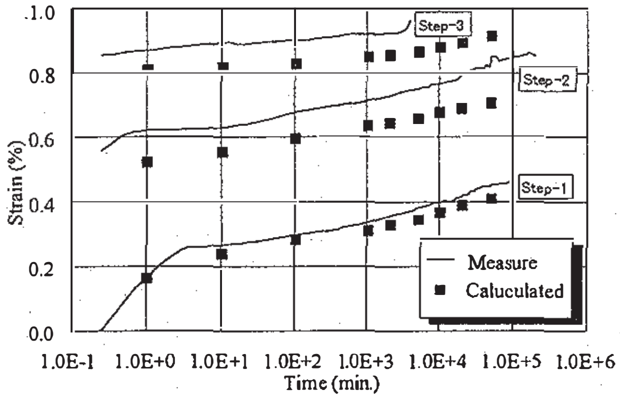

Figure 12 Result of FEM Analysis
(3-Layered : Peak of 2nd Layer)

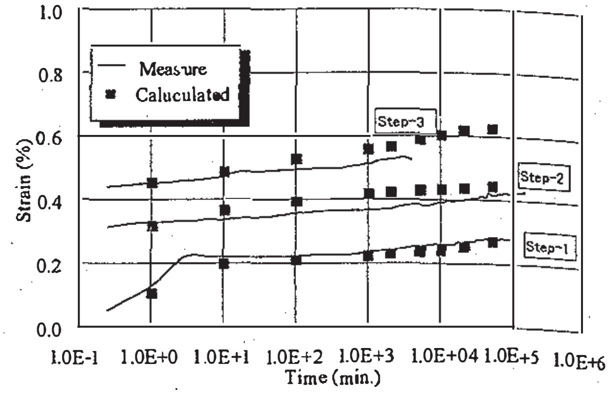

Figure 13 Result of FEM Analysis
(7-Layered : Peak of 4th Layer)

5 CONCLUSIONS

The principal conclusions are as follows:
(1) The deformation of the banking assumed to be due to the creep component caused by long-term loading and the increase in distortion of the geogrid was observed. The increase in distortion as the load was increased was considerable.
(2) The distortion in the geogrid and the creep component were lowest in the model with many layers. Also, the suppression effect of the fill-up ground on the deformation was highest in the model with many layers.
(3) A deformation of the banking assumed to be due to the creep component caused by long-term loading and an increase in distortion of the geogrid was observed, independent of the number of laid layers of geogrid. This increase tended to converge with time.
(4) With this model, no analysis can be made until it fails. However, when considering the load level of reinforced banking; the geogrid can be represented by an appropriate visco-elastic model. This model incorporates creep and can be used to estimate the behavior of reinforcement banking.

REFERENCES

Furuya, H. Toriihara, M. & Hirama, K. 1994. Creep Model Test of Embankment Reinforced with Geo-grids (PART 1) (in Japanese), *The 49th Annual Symposium at Japan Society of Civil Engineers*, pp.1656-1657.

Furuya, H. Toriihara, M. & Hirama, K. 1995. Creep Model Test of Embankment Reinforced with Geo-grids (PART 2) (in Japanese), *The 50th Annual Symposium at Japan Society of Civil Engineers*, pp.1564-1565.

Furuya, H. Toriihara, M. & Hirama, K. 1996. FEM Comparative Analysis of Creep Behavior in a Laboratory Embankment Reinforced with Geogrid (in Japanese), *Proceeding on The 31st Japanese Geotechnical Society*.

Akagi T. 1977. Evaluation of Technique for Visco-Elastic Constants of Leology Model (in Japanese), *Tsuchi to kiso*, Vol.25, No.3, pp.47-52.